

In plane magnetic field and intense laser field effects on second harmonic generation of asymmetric AlGaAs/GaAs double quantum well

J. Pérez-González^a, J. G. Rojas-Briseño^b, F. M. Nava-Maldonado^{c,*}, A. Del Rio-De Santiago^d,
F. Urgan^e, H. Dakhlaoui^{f,g}, and J. C. Martínez-Orozco^a

^a *Unidad Académica de Física, Universidad Autónoma de Zacatecas,
Calzada Solidaridad esquina con Paseo La Bufa S/N. 98060, Zacatecas, Zac., México.*

^b *Unidad Académica de Ciencia y Tecnología de la Luz y la Materia, Universidad Autónoma de Zacatecas,
Carretera Zacatecas-Guadalajara Km. 6, Ejido La Escondida, 98160 Zacatecas, Zac., México.*

^c *Unidad Académica de Ciencias Químicas, Universidad Autónoma de Zacatecas,
Carretera Zacatecas-Guadalajara Km. 6. Ejido la Escondida, C.P. 98160, Zacatecas, Zac., México.*

*e-mail: flavionava@uaz.edu.mx

^d *Unidad Académica de Ingeniería, Universidad Autónoma de Zacatecas,
Ramón López Velarde 801, 98000 Zacatecas, Zac., México.*

^e *Department of Physics, Faculty of Science, Sivas Cumhuriyet University, 58140, Sivas, Turkey.*

^f *Nanomaterials Technology unit, Basic and Applied Scientific Research Center (BASRC), College of Science of Dammam,
Imam Abdulrahman Bin Faisal University, P. O. Box 1982, 31441 Dammam, Saudi Arabia.*

^g *Department of Physics, College of Sciences for Girls,
Imam Abdulrahman Bin Faisal University, Saudi Arabia.*

Received 11 February 2022; accepted 14 April 2022

The optical properties for nano-structured semiconductor systems are of great importance nowadays, due to its possible implementation for the design of efficient optoelectronic devices. It is also well known that external fields can modify the electronic structure and induce changes the optical properties as well. In particular the asymmetric double quantum well structures are of paramount importance because its wide range of possible configurations and also because are experimentally feasible and well controlled, particularly Al_xGa_{1-x}As/GaAs heterostructures. In this work we report a systematic study on second harmonic generation (SHG) for an asymmetric Al_xGa_{1-x}As/GaAs double quantum well, as a function of non-resonant intense laser field and an (*in-plane*) magnetic field. We analyze the energy level behavior as well as the dipole matrix elements as a function of the above mentioned factors, that are important for the SHG, as we discuss in this paper. We report a particular configuration that enhance the SHG signal, with and without intense laser field effect, as well as magnetic fields, that also can be used to tune the SHG.

Keywords: Double quantum wells; Second Harmonic Generation; Intraband transitions; Intense laser field effect.

DOI: <https://doi.org/10.31349/RevMexFis.68.050503>

1. Introduction

The laser discovery, particularly the ruby pulsed one, allowed to P. A. Franken *et al.* in 1961 [1] the second harmonic generation (SHG) experimental observation, the authors reported the observation of the second harmonic at $\lambda = 3472 \text{ \AA}$, while a high intensity monochromatic light of $\lambda = 6943 \text{ \AA}$ hitting on a crystalline quartz sample. For the optical harmonic generation, even of higher orders, nonlinear dielectric coefficients are required, as it is clearly explained by Robert W. Boyd [2] in the traditional book of nonlinear optics. In fact, high intensity fields, as the ones involved in the intense laser physics field, can induce nonlinear dielectric coefficients. In fact, nonlinear optics is interesting and a widely studied topic, from its fundamental as well as from applied point of view. Although we are interested in the SHG, nonlinear optical properties are a rich field of possible effects. For instance, we can mention third order corrections to the absorption coefficient, relative changes in relative refractive index, nonlinear

optical rectification, optical gain, third harmonic generations, among others.

In recent years, an important amount of nonlinear optical properties has been reported in the scientific literature, particularly those related with quantum confinement in which the potential profile asymmetry is present, because this is an important factor for the enhancement of nonlinear optical properties, because the dipole matrix element can be tuned and maximized. For instance, E. Rosencher and Ph. Bois [3], by means of compact density-matrix formalism, report important formulas for the second-order susceptibilities, specifically for the optical rectification and for the SHG and applied these to a step-like asymmetric Al_xGa_{1-x}As/GaAs quantum well (QW) and do the experiments as well, and report good agreement between theoretical model and experimental measurements, reporting an important optical rectification enhancement in comparison with GaAs bulk. P. Boucaud *et al.* [4] performed a detailed SHG analysis for a specific wavelength in Al_xGa_{1-x}As/GaAs asymmetric step-like

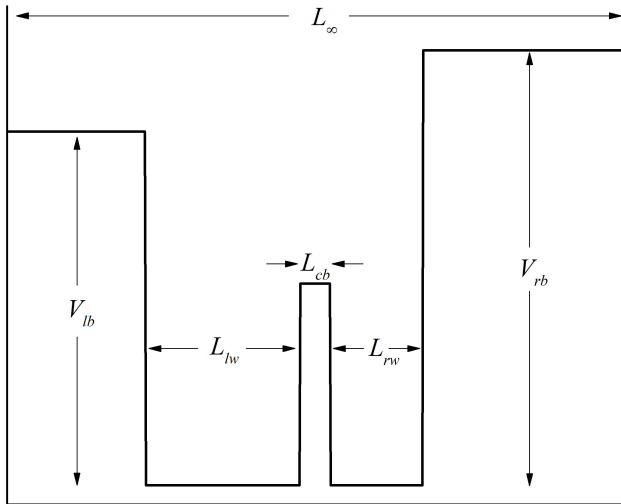


FIGURE 1. Potential profile schematic representation for the asymmetric double $\text{Al}_x\text{Ga}_{1-x}\text{As}/\text{GaAs}$ QW. Here we specified all the involved geometrical parameters used all along the manuscript, except for the central barrier potential height (V_{cb}).

QWs. E. Kasapoglu *et al.* [5] report the absorption coefficient as well as the refractive index change, considering third order nonlinear corrections, with expression obtained in the compact density-matrix, taking into account the effect of external applied electric field. We can give some other references discussing nonlinear optical properties enhancement [6–12].

Now, we would like to talk about the non-resonant intense laser field (ILF) effect, which is an important external factor that can modify the potential profile *seen* by the charge carriers, as reported by F.M.S. Lima *et al.* [13, 14]. In reference [14] the authors consider an ILF polarized perpendicularly to the heterostructure interfaces as well as at sufficiently high frequencies, in such a way that the potential is given by a *laser-dressed* one and concluded that a laser-dressing parameter $\alpha_0 > L/2$, being L the single QW width, transition from single to double QW is predicted. E. Kasapoglu *et al.* [15] also report, that due to ILF effect, the transition from semi-parabolic QW to a kind of asymmetric double QW, affecting importantly the reported nonlinear optical properties, specifically the absorption coefficient and the relative refractive index change. Besides, C. A. Duque *et al.* [16] investigated the combined effects of ILF and externally applied electric field on GaAs exciton states as the ILF modify the potential profile from single to double QW. On the other hand, for the situation $\alpha_0 < L/2$, the potential profile deformation, as reported by E. C. Niculescu *et al.* [17], is an analytical function of α_0 , in fact an $\arccos(\alpha_0)$ one, and they reported the binding energy as well as the density of states for an impurity in a rectangular QW, as a function of the laser-dresser parameter and on the donor impurity position. Also, in this same regime for the laser-dressing parameter ($\alpha_0 < L/2$), E. Kasapoglu *et al.* [5] reported the effect of ILF, electric and magnetic fields on a step-like potential profile on the optical properties, reporting a red-shift in the absorption coefficient and in the relative refractive index change as the intense laser

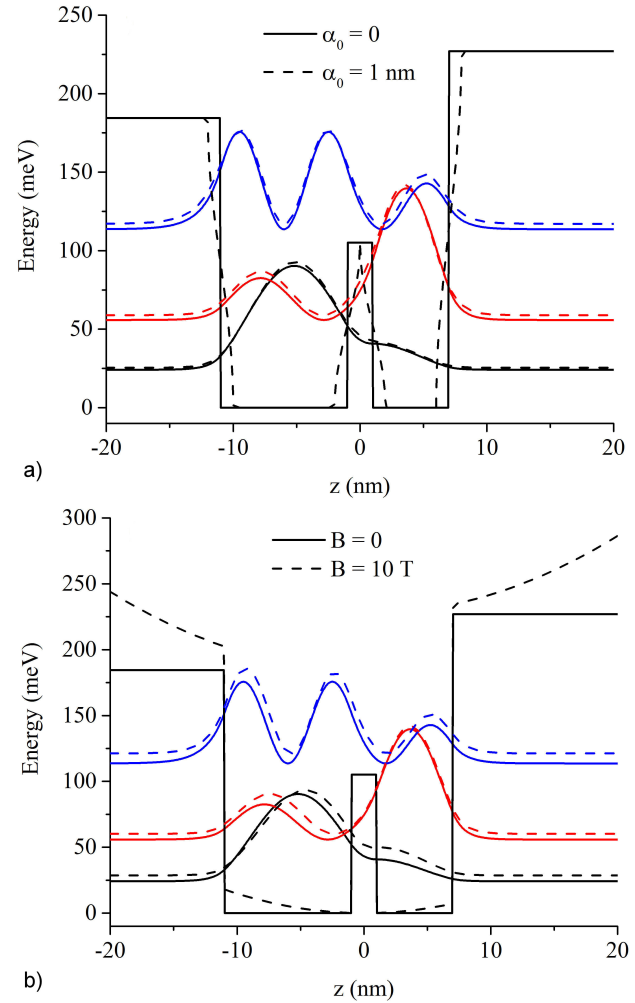


FIGURE 2. Potential profile and electronic structure for asymmetric double $\text{Al}_x\text{Ga}_{1-x}\text{As}/\text{GaAs}$ QW. In a) we depict the electronic structure for zero and $\alpha_0 = 1$ nm ILF effect. In b) the $B = 0$, and $B = 10$ T electronic structure is presented. Ground, first and second excited states, are labeled with black-, red- and blue-lines, respectively.

field effect increase. In general, the asymmetry is provided by different composition in each region of the heterostructure but it is also possible to induce this by external factors as electric and magnetic fields, and in this case also with the non-resonant ILF effect [18–21].

Finally, related with the SHG, as explained in the previous paragraphs, it is present in bulk materials as well as in systems with quantum confinement as reported in Refs. [1–3], as long as the second order susceptibility is different from zero or induced, for example by laser field effects. There exist several reports on this optical property in quantum confined systems. For instance, in 1995, A. Fiore *et al.* [22] carried out the experimental measurement of the SHG for symmetric $\text{AlGaAs}/\text{GaAs}$ QW induced by an externally applied electric field (F) and report the SHG for a GaAs QW width of 50 \AA between $\text{Al}_{0.4}\text{Ga}_{0.6}\text{As}$ barriers with $F = 50 \text{ kV/cm}$ at $\lambda = 1.66 \text{ \mu m}$. From the theoretical point of view, Imen Saidi [23] report the enhancement of SHG in asymmet-

ric AlGaIn/GaN/AlGaIn heterostructure, and reported a significant intensity of the SHG signal. The SHG study as a function of external electromagnetic field for parabolic quantum dots is recently reported in [24]. The enhancement of the SHG for III-Nitride QW by means of metamaterials is studied by N. Nouri and M. Zavvari [25]. Some other recent reports on the SHG [26, 27], and references therein.

In this paper we systematically studied the combined effect of the ILF, in the $\alpha_0 < L/2$ regime, here L represents the narrower potential profile region, being in this case the central barrier width L_{cb} (see Fig. 1, where all the geometrical parameters are depicted), and an *in-plane* (x -directed) magnetic field on double asymmetric $\text{Al}_x\text{Ga}_{1-x}\text{As}/\text{GaAs}$ QW with the aim to enhance the SHG response by identifying the the geometric parameters that generate the resonance condition and considering the effect of the external fields.

The organization of the paper is the following: In Sec. 2 we introduce the implemented theoretical framework, then Sec. 3 shows the results and discussion, and finally the main conclusions are given in Sec. 4.

2. Theoretical Framework

In this paper we report the electronic structure as well as the SHG for asymmetric $\text{Al}_x\text{Ga}_{1-x}\text{As}/\text{GaAs}$ double quantum well (ADQW) considering a high frequency, non-resonant, ILF effect and an in-plane (x -directed) magnetic field. This was done within the effective mass approximation and the conduction band offsets are computed by using the solid model theory (SMT) [28, 29].

The time-independent Schrödinger equation of the system is given by:

$$\left[-\frac{\hbar^2}{2m_e^*} \frac{d^2}{dz^2} + \frac{e^2 B^2}{2m_e^* c^2} z^2 + \langle V(z; \alpha_0) \rangle \right] \psi_n(z) = E_n \psi_n(z), \quad (1)$$

here \hbar stands for the reduced Planck constant, m_e^* is the electron effective mass for each material, e is electron charge and B represent the magnetic field strength. As we already mentioned, in this paper we implemented the Van de Walle's Solid Model Theory (SMT) [28] in order to determine the heterostructure band-offsets for the $\text{Al}_x\text{Ga}_{1-x}\text{As}/\text{GaAs}$ ADQW, because this formalism consider the strain due to heterostructure lattice mismatch. In the paper of P. Zhang and coworkers [29], and references therein, we can find the main expressions for this method to be implemented and the involved parameters are given in Table I.

As described in Table I caption, here we are taking into account the bowing parameter for the $\text{Al}_x\text{Ga}_{1-x}\text{As}$ energy band-gap, given as:

$$E_g^{\text{AlGaAs}}(x) = (x)E_g^{\text{AlAs}} + (1-x)E_g^{\text{GaAs}} + x(1-x)b, \quad (2)$$

TABLE I. Computed parameters in the model solid theory for the constituent materials using the Vegard's law for $\text{Al}_x\text{Ga}_{1-x}\text{As}$, except for the E_g where the bowing parameter is considered.

	$\text{Al}_{0.15}\text{Ga}_{0.85}\text{As}$	$\text{Al}_{0.25}\text{Ga}_{0.75}\text{As}$	$\text{Al}_{0.30}\text{Ga}_{0.70}\text{As}$
ε_r (e)	12.474	12.190	12.048
a (nm)	0.565	0.565	0.565
E_g (eV)	1.618	1.756	1.828
Δ_{so} (eV)	0.332	0.326	0.323
$E_{v,av}$ (eV)	-7.005	-7.062	-7.091
V_c (meV)	105.17	184.54	227.00

here $b = -0.37$ stands for the deviation of the well known Vegard's law linear interpolation. The structural potential profile $V_c(z)$ is an ADQW, depicted in Fig. 2 with continuous black solid-lines, that will be affected by the considered external factors. In Fig. 2 we present the effect of the laser dressing-parameter a) and the magnetic field b) on the potential profile as well as on the probability amplitudes for the ground (black-lines), first excited (red-lines) and second excited (blue-lines) states, for the chosen values specified in the figure. When we consider the ILF effect in the high frequency limit the electron is subject to a time-averaged potential [13, 14]:

$$\langle V(z; \alpha_0) \rangle = \frac{\Omega}{2\pi} \int_0^{2\pi/\Omega} V_c(z + \alpha_0 \sin \Omega t) dt. \quad (3)$$

The laser-dressing parameter α_0 is defined as:

$$\alpha_0 = \frac{eA_0}{m_e^* \Omega}, \quad (4)$$

where Ω and A_0 stands for the frequency and the amplitude of the potential vector of the laser field, respectively.

The method that we use to solve the Eq. (1) is the well-known diagonalization procedure. So, by expanding the envelope function as follow,

$$\psi_n(z) = \sqrt{\frac{2}{L_\infty}} \sum_{m=1}^{\infty} C_m \sin \left(\frac{m\pi}{L_\infty} z + \frac{m\pi}{2} \right), \quad (5)$$

we can compute the Hamiltonian matrix for the Hamiltonian in Eq. (1) $H_{mn} = \langle \psi_m | H | \psi_n \rangle$, that include the matrix elements for kinetic energy term, the quadratic potential profile due to the in-plane magnetic field as well as the laser dressing potential matrix elements that considers the double QW confinement potential, and after diagonalize this matrix we obtain the c_m coefficients and the energies E_n . Here L_∞ stands for the infinite barrier rectangular QW width, of the complete orthonormal set for the envelope function expansion. Besides Eq. (5) has an infinite sum of terms, from the physical point of view is necessary just a matrix that ensures the energy convergency, that in this case is for $n = 100$.

Once computed the electronic structure for the system, the dipole matrix element is given by:

$$M_{ij} = \langle \psi_i(z) | z | \psi_j(z) \rangle, \quad (6)$$

that allows to compute the coefficients corresponding to the susceptibility of second order that give the SHG, being $\psi_i(z)$ and $\psi_j(z)$ the initial and final states, following the lines of E. Rosencher and Ph. Bois [3]:

$$\chi_{2\omega}^{(2)} = \frac{e^3 \rho}{\varepsilon_0} \frac{|M_{01} M_{12} M_{20}|}{(\hbar\omega - E_{10} - i\hbar\Gamma_j)(2\hbar\omega - E_{20} + i\hbar\Gamma_j)}, \quad (7)$$

where ε_0 is the vacuum permittivity, ρ represent the system charge density, ω stands for the incident photon angular frequency and $\hbar\Gamma_j = \hbar/T_j$ are the damping terms associated with the mean lifetime due to intraband dispersion rate. Finally, the energy differences are given $E_{ji} = (E_j - E_i)$. We must stress here that the SHG is generated by an extra laser, not the one that induces the laser-dressing potential, but a resonant one.

3. Results and discussion

Electronic properties as well as SHG results are presented and discussed in this section for $\text{Al}_x\text{Ga}_{1-x}\text{As}/\text{GaAs}$ ADQW. As mentioned in the previous section, we are working within the effective mass approximation and the band-offsets are determined by means of the model solid theory, with the parameters listed in Table I. The chosen aluminum concentration (x) for the left-, central- and right-hand barriers are: 0.25, 0.15 and 0.30, respectively. On the other hand, the right-hand well width is fixed to $L_{rw} = 6.0$ nm with a central barrier of $L_{cb} = 2$ nm. In the following, we will present the results as a function of L_{lw} , ranging from 2 up to 16 nm, and as a function of the in-plane (x -directed) magnetic field of strength B , with and without intense laser field effect.

In Fig. 3a) is shown $(E_1 - E_0)$ as well as the value of $(E_2 - E_0)/2$ for the system as a function of the left-hand side QW L_{lw} , without any ILF (black solid lines) and with a laser-dressing parameter of $\alpha_0 = 1$ nm (blue dashed lines). Figure 3b) shown the same energy differences, but in this case for $B = 0$ (black solid lines), $B = 5$ T (red dash-dot lines) and $B = 10$ T (blue dash-dot-dot lines). The aim of this study was to determine the intersection of both quantities that makes the SHG, given by Eq. (7), to be a sharp function. The first crossing in 3a) can be observed for L_{lw} about 2.8 nm (at 72 meV) and 2.9 (at 71 meV) for $\alpha_0 = 0$ and $\alpha_0 = 1$ nm, respectively. Then, as L_{lw} increases, we observe a second crossing at L_{lw} about 13.8 nm (at 31 meV) and 13.7 (at 32 meV), for the same values of α_0 , and we can clearly see that the ILF slightly modify the energy levels. Now, in Fig. 3b) we report these curves for $B = 0$, that has the same crossing as for $\alpha_0 = 0$; Then, with red dash-dot lines, we present the results for $B = 5$ T and we observe that the first energy crossing is for a smaller L_{lw} value and it experiences a blueshift, and the second energy crossing increase further in

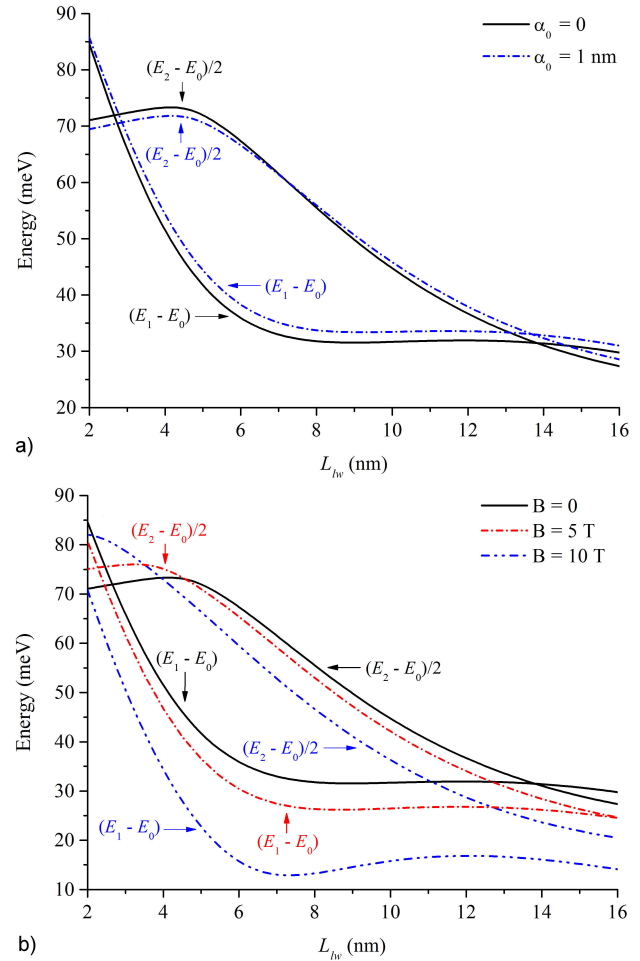


FIGURE 3. Main energy level difference $(E_1 - E_0)$ as well as the value of $(E_2 - E_0)/2$ for the ADQW as a function of the left-hand side QW width L_{lw} . In a) we present these for $\alpha_0 = 0$ and $\alpha_0 = 1$ nm, while in b) these are shown for $B = 0$, $B = 5$ T and $B = 10$ T.

the L_{lw} QW width but now with a redshift; Finally we report the case for $B = 10$ T, in the region of $L_{lw} \in [2, 16]$ and there is not any energy crossing, that will imply that the SHG resonant condition will not be fulfilled, at least not for chosen set of parameters.

Dipole matrix elements (DME) $|M_{ij}|$ and the product of them $|M_{10}M_{12}M_{20}|$, as a function of L_{lw} , taking into account ILF effects (α_0) and external magnetic field (B) are shown in Fig. 4. In Fig. 4a), the DME for the main transition $|M_{10}|$ is represented with black lines, the intermediate one $|M_{12}|$ with red lines, while the second to ground state $|M_{20}|$ is given with blue ones. In Fig. 4b) the product of them is shown (in all the cases the continuous line is for $\alpha_0 = 0$ and dashed ones for $\alpha_0 = 1$ nm). Observe that, in general, the ILF effect slightly modify the DME behavior and that the factor $|M_{10}M_{12}M_{20}|$ start to increase for $L_{lw} > 6$ nm, all this is for $B = 0$. On the other hand, with $\alpha_0 = 0$, in Fig. 4c) we present $|M_{ij}|$ for $B = 0$ (continuous line), 5 T (dashed line), and 10 T (point-dashed lines), with the same color-code as in Fig. 4a) for the involved DME, while in Fig. 4d) the product

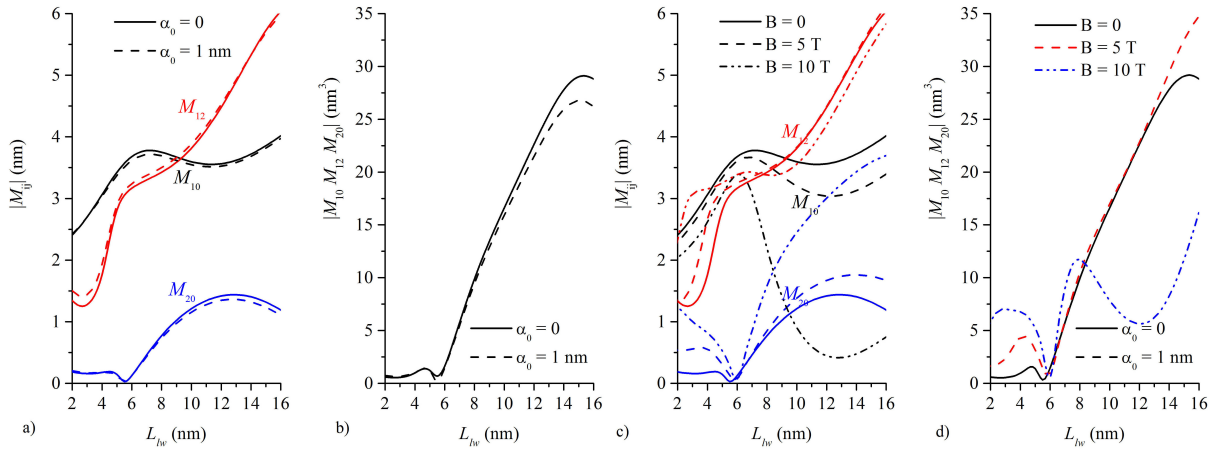


FIGURE 4. Dipole matrix elements $|M_{ij}|$ in a) and c), and the product of them $|M_{10}M_{12}M_{20}|$ in b) and d), as a function of the left-hand side QW width L_{lw} . In the first line plot, this is shown for $\alpha_0 = 0$ and for $\alpha_0 = 1$ nm, while in the second one these are for $B = 0, 5,$ and 10 T.

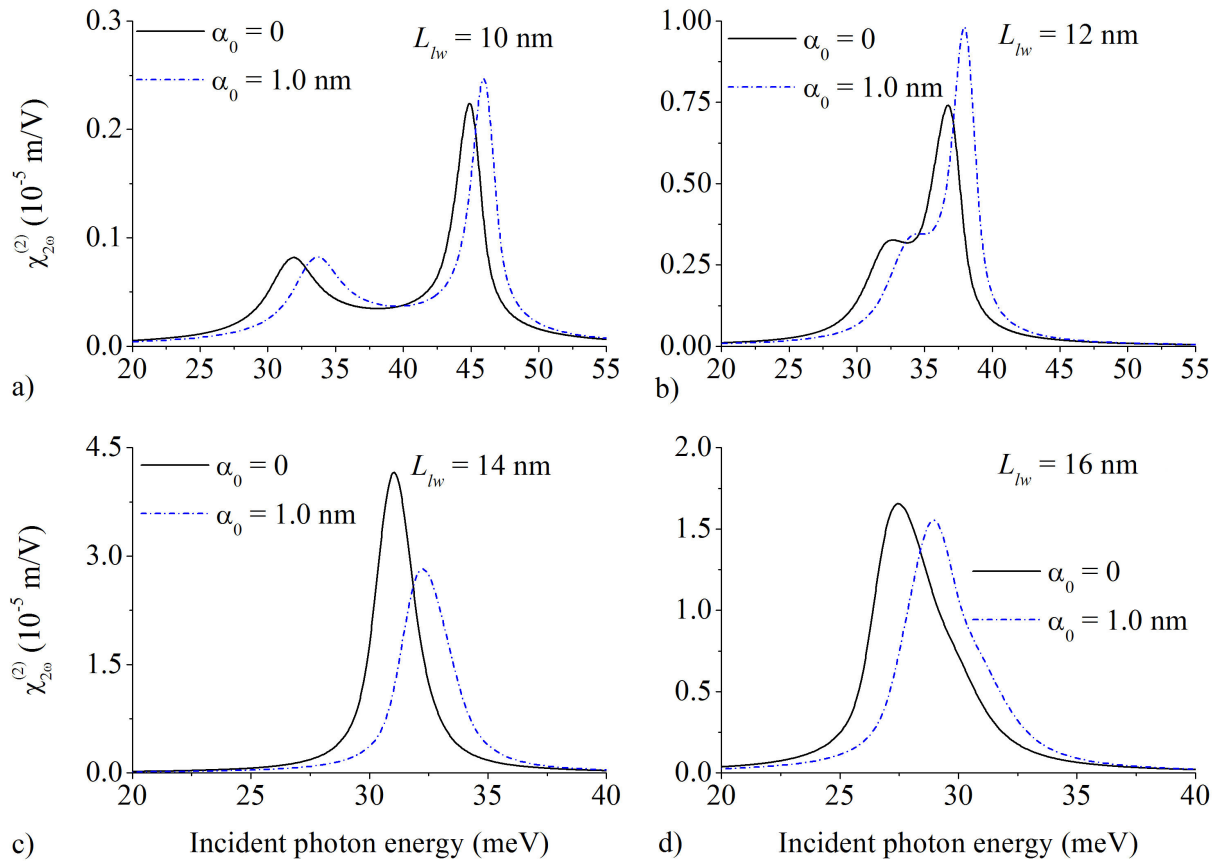


FIGURE 5. Second harmonic generation for the system as a function on the incident photon energy, for L_{lw} with values of; a) 10 nm, b) 12 nm, c) 14 nm, and 16 d) nm, without ILF effect (continuous line) and with $\alpha_0 = 1$ nm (point-dashed line).

of them is shown. In this case we can see that the magnetic field has a more pronounced effect on individual DME that strongly affect the product of them $|M_{10}M_{12}M_{20}|$, and eventually will be reflected in the SHG signal. In general, the $|M_{20}|$ vanishes for L_{lw} about 5.5 nm because the the envelope functions of the ADQW are nearly symmetric, and this becomes important for $L_{lw} > 6$ nm, except in the case of

$B = 10$ T that becomes minimum for L_{lw} around 12 nm, that is due to the strong fall in the $|M_{10}|$ value and, as we will analyze in the following, this has important implications in the SHG behavior.

Figure 5 shows second harmonic generation for the system considering the ILF effect, as a function of the incident photon energy, for four values of L_{lw} ; a) 10 nm, b) 12 nm,

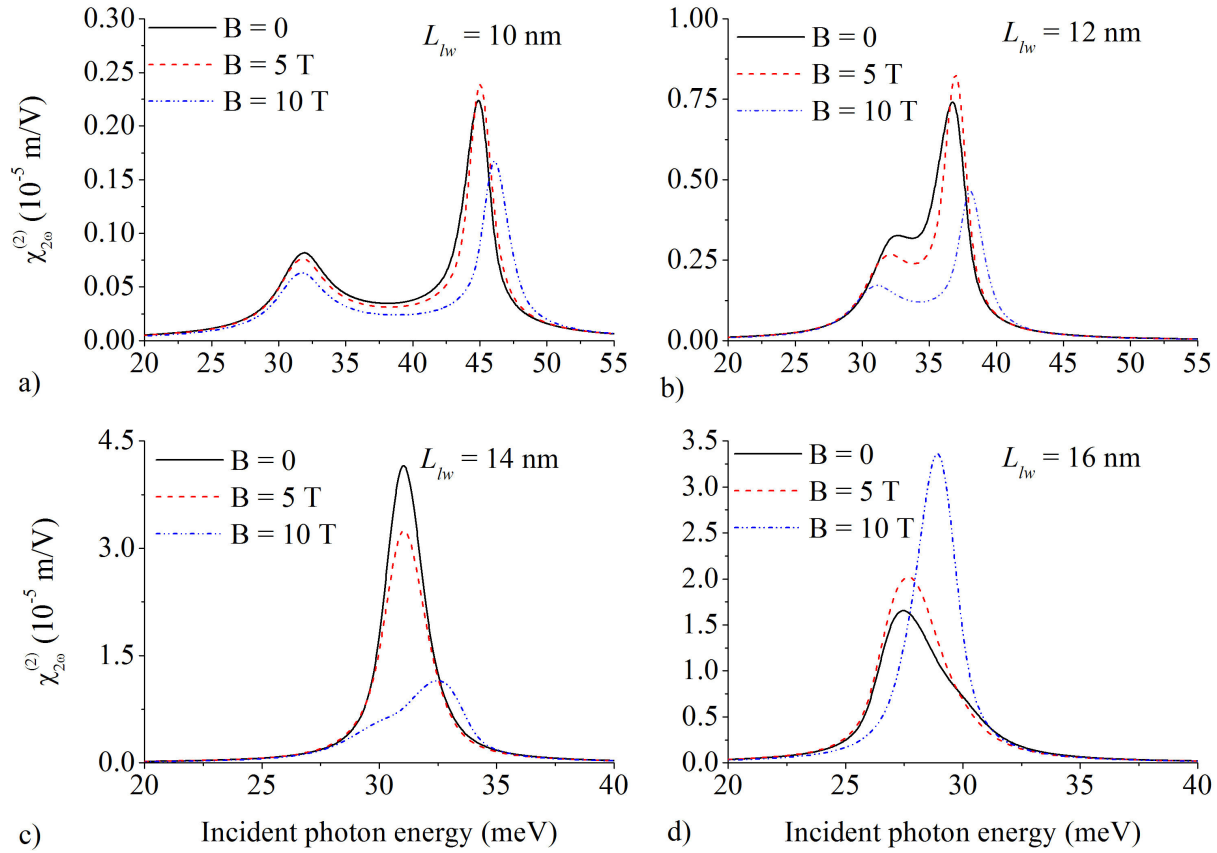


FIGURE 6. Second harmonic generation for the system, as a function of incident photon energy, for the same set of L_{lw} values as in the previous figure, when an external magnetic field is considered.

c) 14 nm, d) and 16 nm, that are within the region of higher values for the dipole matrix element product $|M_{10}M_{12}M_{20}|$ and include the second energy level crossing, as a function of L_{lw} , as shown in Figs. 3a) and 4b). The SHG is given by Eq. (7), as reported by E. Rosencher and Ph. Bois [3], that is formally defined when the energy difference of the first excited and ground state coincides with the energy difference from second excited state and the first excited one, in this case the energy crossing in Fig. 3. Out of this condition, this can be interpreted as a sum-frequency generation, as defined by Robert W. Boyd [2]. So, in Fig. 5a) we report the results for $L_{lw} = 10$ nm and we observe two peaks because the energy level difference do not coincide and the ILF effect characterized with $\alpha_0 = 1$ nm induces a blueshift in the curve. In Fig. 5b), for $L_{lw} = 12$ nm, the two peaks become closer and the intensity increases almost four times with the shift toward higher energies due to ILF effects. In Fig. 5c) we show the results for $L_{lw} = 14$ nm, that is very close to the energy difference crossing, where the SHG condition is fulfilled, and it is clear that the amplitude is much more important, and that the ILF effect keep the blueshift but the amplitude decreases. Finally, in Fig. 5d) we can see that an small shoulder about 30 meV in the incident photon energy, in both cases, and the magnitude start to decrease. Finally, it is clearly seen from those four figures that the SHG peak shifts towards lower energies with the increase of the QW width.

Figure 6 show the effect of the *in-plane* external magnetic field on the SHG for the system, with the same set of parameters used in the previous figure, with $\alpha_0 = 0$. In Fig. 6a), with $L_{lw} = 10$ nm, the applied magnetic field, with values of 5 and 10 T, induces small changes in the shape of the SHG signal in comparison with the $B = 0$ situation. For $L_{lw} = 12$ nm, depicted in Fig. 6b), we can see a more important diminishing in the SHG signal due to the applied magnetic field. The most interest case is given in Fig. 6c), that corresponds to $L_{lw} = 14$ nm, where we can observe a quenching tendency in the SHG signal for $B = 10$ T, that allows to state that the SHG signal can be attenuated or even turns of by the effect of the magnetic field. Finally, when L_{lw} reaches the value of 16 nm, as can be seen in Fig. 6d), the magnetic field importantly enhance the SHG signal, followed with a blue-shift in the SHG peak.

4. Conclusions

In this paper we report a second harmonic generation systematic study for an asymmetric $\text{Al}_x\text{Ga}_{1-x}\text{As}/\text{GaAs}$ QW well as a function of non-resonant intense laser field effect and an (*in-plane*) magnetic field. For the chosen set of parameters, without intense laser field effects and any magnetic field B , we found two energy level crossing (resonances) but only

the second one, for L_{lw} about 14 nm has large values on the dipole matrix element product $|M_{10}M_{12}M_{20}|$, that importantly enhance for $L_{lw} > 6$ nm, that are fundamental for the second harmonic generation. We can conclude that the intense laser field effect, although it seems that it does not affect the dipole matrix elements so much, has noticeable blue-shift correction in the second harmonic generation signal, that importantly affect the amplitude, particularly near the energy level crossing. The most important effect on the second harmonic generation signal is due to the *in-plane* (x -directed) applied magnetic field because, as we can be seen from our results, this significantly affect the dipole matrix elements $|M_{ij}|$ as well as the energy level structure, that have noticeable effect on the optical properties. In this paper we

state that for the chosen set on parameters, that are within the experimental feasible ones, the magnetic field can be used to enhance the second harmonic generation signal or even as mechanism to inhibit this one, that can be used as a switching mechanism.

Acknowledgements

J.C. Martínez-Orozco acknowledge to CONACyT-SEP México for the partially financial support through the *Fondo sectorial de investigación para la educación* with project number A1-S-8842 entitled “*Estudio de propiedades optoelectrónicas básicas en pozos, puntos y anillos cuánticos de materiales III-V y II-VI y sus heteroestructuras*”.

1. P. A. Franken, A. E. Hill, C. W. Peters, and G. Weinreich. Generation of Optical Harmonics. *Phys. Rev. Lett.* **7** (1961) 118.
2. Robert W. Boyd. *Nonlinear Optics, Third Edition*. Academic Press, Inc., USA, 3rd edition, 2008.
3. E. Rosencher and Ph. Bois. Model system for optical nonlinearities: Asymmetric quantum wells. *Phys. Rev. B*, **44** (1991) 11315.
4. P. Boucaud, F. H. Julien, D. D. Yang, J-M. Lourtioz, E. Rosencher, P. Bois, and J. Nagle. Detailed analysis of second-harmonic generation near $10.6\mu\text{m}$ in GaAs/AlGaAs asymmetric quantum wells. *Appl. Phys. Lett.*, **57** (1990) 215.
5. E. Kasapoglu, C.A. Duque, M.E. Mora-Ramos, R.L. Restrepo, F. Urgan, U. Yesilgul, H. Sari, and I. Sökmen. Combined effects of intense laser field, electric and magnetic fields on the nonlinear optical properties of the step-like quantum well. *Mater. Chem. Phys.*, **154** (2015)170.
6. H. Yildirim and M. Tomak. Optical absorption of a quantum well with an adjustable asymmetry. *Eur. Phys. J. B.*, **50** (2006) 559.
7. A. Rostami, H. Baghban Asghari Nejad, and H. Rasooli Saghai. Highly enhanced second-order nonlinear susceptibilities in tailored GaN–AlGaN–AlN quantum well structures. *Physica B*, **403** (2008) 2725.
8. Xin Liu, LiLi Zou, Chenglin Liu, Zhi-Hai Zhang, and Jian-Hui Yuan. The nonlinear optical rectification and second harmonic generation in asymmetrical Gaussian potential quantum well: Effects of hydrostatic pressure, temperature and magnetic field. *Opt. Mater.*, **53** (2016) 218.
9. F.M. Nava-Maldonado, J.G. Rojas-Briseño, J.C. Martínez-Orozco, and M.E. Mora-Ramos. Strain effects in the absorption coefficient and relative refractive index change in double asymmetric $\text{Al}_x\text{Ga}_{1-x}\text{N}/\text{GaN}$ quantum wells. *Physica E*, **111** (2019) 134.
10. Raktim Sarma, Domenico de Ceglia, Nishant Nookala, Maria A. Vincenti, Salvatore Campione, Omri Wolf, Michael Scalora, Michael B. Sinclair, Mikhail A. Belkin, and Igal Brener. Broadband and Efficient Second-Harmonic Generation from a Hybrid Dielectric Metasurface/Semiconductor Quantum-Well Structure. *ACS Photonics*, **6** (2019) 1458.
11. Sofia Evangelou. Nonlinear optical absorption coefficient and refractive index change in symmetric semiconductor nanostructures: Comparison between different methods. *Physica E*, **124** (2020) 114307.
12. J C Martínez-Orozco, F Urgan, and K A Rodríguez-Magdaleno. Studies on the nonlinear optical properties of two-step GaAs/Ga $_{1-x}$ Al $_x$ As quantum well. *Phys. Scr.*, **95** (2020) 035802.
13. B. G. Enders, F. M. S. Lima, O. A. C. Nunes, A. L. A. Fonseca, D. A. Agrello, Fanyao Qu, E. F. Da Silva, and V. N. Freire. Electronic properties of a quasi-two-dimensional electron gas in semiconductor quantum wells under intense laser fields. *Phys. Rev. B*, **70** (2004) 035307.
14. F. M. S. Lima, M. A. Amato, O. A. C. Nunes, A. L. A. Fonseca, B. G. Enders, and E. F. da Silva. Unexpected transition from single to double quantum well potential induced by intense laser fields in a semiconductor quantum well. *J. Appl. Phys.*, **105** (2009) 123111.
15. E. Kasapoglu, C. A. Duque, H. Sari, and I. Sökmen. Intense laser field effects on the linear and nonlinear intersubband optical properties of a semi-parabolic quantum well. *Eur. Phys. J. B*, **82** (2011) 13.
16. C. A. Duque, M. E. Mora-Ramos, E. Kasapoglu, H. Sari, and I. Sökmen. Combined effects of intense laser field and applied electric field on exciton states in GaAs quantum wells: Transition from the single to double quantum well. *phys. status solidi B*, **249** (2012) 118.
17. E.C. Niculescu, L.M. Burileanu, and A. Radu. Density of impurity states of shallow donors in a quantum well under intense laser field. *Superlattice. Microst.*, **44** (2008) 173.
18. M.E. Mora-Ramos, C.A. Duque, E. Kasapoglu, H. Sari, and I. Sökmen. Electron-related nonlinearities in GaAs-Ga $_{1-x}$ Al $_x$ As double quantum wells under the effects of intense laser field and applied electric field. *J. Lumin.*, **135** (2013) 301.
19. M.J. Karimi and H. Vafaei. Intense laser field effects on the linear and nonlinear intersubband optical properties in a strained InGaN/GaN quantum well. *Physica B*, **452** (2014) 131.

20. J.C. Martínez-Orozco, J.G. Rojas-Briseño, K.A. Rodríguez-Magdaleno, I. Rodríguez-Vargas, M.E. Mora-Ramos, R.L. Restrepo, F. Urgan, E. Kasapoglu, and C.A. Duque. Effect of the magnetic field on the nonlinear optical rectification and second and third harmonic generation in double δ -doped GaAs quantum wells. *Physica B*, **525** (2017) 30.
21. U. Yesilgul, H. Sari, F. Urgan, J.C. Martínez-Orozco, R.L. Restrepo, M.E. Mora-Ramos, C.A. Duque, and I. Sökmen. Effects of electromagnetic fields on the nonlinear optical properties of asymmetric double quantum well under intense laser field. *Chem. Phys.*, **81** (2017) 485.
22. A. Fiore, E. Rosencher, V. Berger, and J. Nagle. Electric field induced interband second harmonic generation in GaAs/AlGaAs quantum wells. *Appl. Phys. Lett.*, **67** (1995) 3765.
23. Imen Saidi. Single- and double-resonant enhancement of second-harmonic generation in asymmetric AlGaIn/GaN/AlGaIn quantum well heterostructures. *J. Appl. Phys.*, **125** (2019) 185702.
24. Liangcheng Zhang, Xuechao Li, Xinge Liu, and Zirui Li. The influence of second-harmonic generation under the external electric field and magnetic field of parabolic quantum dots. *Physica B*, **618** (2021) 413197.
25. Neda Nouri and Mahdi Zavvari. Second-Harmonic Generation in III-Nitride Quantum Wells Enhanced by Metamaterials. *IEEE Photon. Technol. Lett.*, **28** (2016) 2199.
26. M.J. Karimi and H. Vafaei. Second-order nonlinear optical properties in a strained InGaN/AlGaIn quantum well under the intense laser field. *Superlattice. Microst.*, **78** (2015) 1.
27. Kun-Ching Shen, Yi-Teng Huang, Tsung Lin Chung, Ming Lun Tseng, Wei-Yi Tsai, Greg Sun, and Din Ping Tsai. Giant Efficiency of Visible Second-Harmonic Light by an All-Dielectric Multiple-Quantum-Well Metasurface. *Phys. Rev. Appl.* **12** (2019) 064056.
28. Chris G. Van de Walle. Band lineups and deformation potentials in the model-solid theory. *Phys. Rev. B*, **39** (1989) 1871.
29. Peng Zhang, Yanrong Song, Jinrong Tian, Xinpeng Zhang, and Zhigang Zhang. Gain characteristics of the InGaAs strained quantum wells with GaAs, AlGaAs, and GaAsP barriers in vertical-external-cavity surface-emitting lasers. *J. Appl. Phys.* **105** (2009) 053103.